and-substitution reactions of the trinuclear complexes, it is not possible to further discuss these interesting findings.

Acknowledgment. We thank the Instrument Center, the Institute for Molecular Science, for assistance in obtaining the XPS spectra. We also thank Japan Analytical Industry Co. Ltd., for the preparative liquid chromatography, and Professor Y. Shono and Dr. K. Kusaba (Research Institute for Iron, Steel, and Other Metals, Tohoku University), for the measurements of the X-ray powder diffraction patterns.

Photoactivation of Metal Oxide Surfaces: Photocatalyzed Oxidation of Alcohols by Heteropolytungstates

Marye Anne Fox,* Raul Cardona, and Elizabeth Gaillard

Contribution from the Department of Chemistry, The University of Texas at Austin, Austin, Texas 78712. *Received January 9, 1987. Revised Manuscript Received May 20, 1987*

Abstract: Photoinduced oxidation of primary, secondary, and tertiary alcohols by several tungstates of varying structural complexity ($WO_2(OR)_2$, $PW_{12}O_{40}^{3-}$, or $(WO_3)_n$) requires strong alcohol precomplexation before photoactivation and occurs via a rapid two-electron transfer, in contrast to previous mechanistic suggestion. The relative efficiencies for alcohol oxidation induced by excitation of a series of heteropolytungstates of increasing molecular complexity are reported. Mechanistic features of the photocatalytic oxidation are described, and a comparison is drawn between thermal and photochemical activation of the heteropolytungstates.

A fundamental problem in catalysis is to identify and characterize reactions that can be induced by heat or by light. Contrasting chemical behavior observed upon thermal or photochemical activation can provide information valuable in understanding surface–solute interactions and the effect of the catalyst on relative activation energies of competing pathways. Recent reports of photocatalytic oxidation of organic substrates on heteropolyoxoanions excited by ultraviolet wavelengths,[1-11] together with previous reports of thermal oxidative catalysis on these same substrates,[12-14] make this family of compounds an attractive target for such mechanistic investigations. Furthermore, our interest in the nature of fundamental interactions of organic molecules on the surfaces of irradiated metal oxide semiconductors[15,16] has led us to investigate the photocatalytic reactions of these species as soluble analogues of semiconductor metal oxide suspensions.

Transition-metal oxides represent species that span the range from discrete molecules to extended semiconductor structures. As a subset of this class, the polyoxoanions possess structures that are well characterized at the molecular level[13,14] and acidity and redox properties that can be systematically controlled. The heteropolyoxometalates consist of a single atom (P, Si, Co, etc.) surrounded by metal oxide units, constituting arrays that may contain up to 200 or more atoms. For the usual oxidation levels

Table I. Heteropolyoxoanions Evaluated as Photocatalysts

cation	central atom[a]	size
$H_3PW_{12}O_{40}\cdot 30H_2O$	$Na_3PW_{12}O_{40}\cdot 10H_2O$	$WO_2(OR)_2$
$Na_3PW_{12}O_{40}\cdot 10H_2O$	$Na_6H_2W_{12}O_{40}\cdot 22H_2O$	$Na_3PW_{12}O_{40}\cdot 10H_2O$
$(NH_4)_3PW_{12}O_{40}\cdot 10H_2O$	$K_4SiW_{12}O_4\cdot 8H_2O$	$(NH_4)_6P_2W_{18}O_{62}\cdot 30H_2O$
$(Pr_4N)_3PW_{12}O_{40}\cdot 10H_2O$	$H_5(FeW_{12}O_{40})\cdot 10H_2O$	$(NH_4)_{14}NaP_5W_{30}O_{110}\cdot 31H_2O$
	$K_5HCoW_{12}O_{40}\cdot 15H_2O$	$(Bu_4N)_5H_4P_2W_{15}V_3O_{62}$[b]
		$(Bu_4N)_4H_3SiW_9V_3O_{40}$[b]
		$(WO_3)_n$[c]
		$(WO_3)_n$/Pt

[a] The band gap of WO_3 is close to 2.7 eV, which corresponds approximately to 459 nm.[46] [b] These samples were a gift from R. G. Finke, University of Oregon. [c] Reference 46.

Table II. Solubility of Salts of **1**

solvent	salt: Na^+ ($\cdot H_2O$) rt[a]/Δ	NH_4^+ ($\cdot H_2O$) rt/Δ	Pr_4N^+ ($\cdot H_2O$) rt
water	PS/S[b]	I/S	I
ether	I/I	I/I	I
acetone	PS/PS	I/I	I
1,4-dioxane	I/I	I/I	I
acetonitrile	PS/PS	I/I	S
CCl_4	I/–	I/–	I
$CHCl_3$	I/–		
CH_2Cl_2	I/I	PS/PS	I
acetic anhydride	I/I	I/I	
DMF	PS/PS	PS/S	S
DMSO	S (yellow)/S	I/S (after a day)	S (yellow)
pyridine	C/PS, C	C/I	
methanol	S/S	I/I	I
ethanol	PS/PS	I/I	

[a] rt = room temperature. [b] S = soluble; PS = partially soluble; I = insoluble; C = cloudy.

(1) Papaconstantinou, E. *Chem. Commun.* **1982**, 12.
(2) Papaconstantinou, E.; Dimotikali, D.; Politou, A. *Inorg. Chim. Acta* **1980**, *43*, 155.
(3) Darwent, J. R. *Chem. Commun.* **1982**, 798.
(4) Papaconstantinou, E.; Dimotikali, D. *Inorg. Chim. Acta* **1984**, *87*, 177.
(5) Ward, M. D.; Brazdil, J. F.; Graselli, R. K. *J. Phys. Chem.* **1984**, *88*, 4210.
(6) Yamase, T.; Kurozumi, T. *J. Chem. Soc., Dalton Trans.* **1983**, 2205.
(7) Yamase, T. *Inorg. Chim. Acta* **1981**, *54*, L207.
(8) Yamase, T. *J. Synth. Org. Chem. Jpn.* **1985**, *43*, 249.
(9) Renneke, R. F.; Hill, C. L. *J. Am. Chem. Soc.* **1986**, *108*, 3528.
(10) Argitis, P.; Papaconstantinou, E. *J. Photochem.* **1985**, *30*, 445.
(11) Hill, C. L.; Bouchard, D. A. *J. Am. Chem. Soc.* **1985**, *107*, 5148.
(12) Kozhevnikov, I. V.; Matveev, K. I. *Russ. Chem. Rev. (Engl. Transl.)* **1982**, *51*, 1075.
(13) Pope, M. T. *Heteropoly and Isopoly Oxometalates*; Springer-Verlag: New York, 1983.
(14) Day, V. W.; Klemperer, W. G. *Science (Washington, D.C.)* **1985**, *228*, 533.
(15) Fox, M. A. *Acc. Chem. Res.* **1983**, *16*, 314.
(16) Fox, M. A. *NATO Adv. Sci. Inst. Ser.* **1986**, *174*, 363.

0002-7863/87/1509-6347$01.50/0

Table III. Dependence of the Absorption Maximum of **1** (Sodium Salt) on Solvent

solvent	λ_{max},[a] nm
H_2O	255
H_2O (pH <1)	263
CH_3CN	263
DMF	267
DMSO	266

[a] ±2 nm.

of the transition metal, multiple-electron reductions can be observed,[10,18] and in some cases, i.e., in $PW_{12}O_{40}^{3-}$ and other species that exist as polyanions of crystallographically imposed threefold symmetry (Keggin structures),[17] minimal structural changes accompany these reductions. The resulting thermally stable reduced ions have extensive analytical applications consequent to their intense blue coloration. The reduced polytungstates can be easily reoxidized,[1] a feature necessary for catalytic applications.

We hoped to examine with photochemical techniques several members of this family as models for the molecule-to-solid state continuum to determine whether the degree of aggregation can influence photocatalytic activity. We report here evidence that in a series of tungstates of increasing molecular complexity photoreactivity characteristic of light-induced charge separation occurs only when preceded by effective precomplexation of the substrate and the metal oxide. We also discuss the mechanism for alcohol oxidation and its relationship to the general problem of light-induced multiple-electron exchange. Finally, a comparison between thermal and photochemical catalytic activity is drawn. In our mechanistic studies we focus on the oxidation chemistry induced by excited $NaPW_{12}O_{40}^{3-}$ (**1**) but also include spectra and relative reactivity data for several structurally related complexes in order to survey the potential for employing structurally modified photocatalysts in future studies.

Polytungstate Photocatalysts

The three series of heteropolytungstates shown in Table I were synthesized by known procedures[19-25] for evaluation as photocatalysts. We have adopted $PW_{12}O_{40}^{3-}$ (**1**) as our reference polyoxoanion. In column 1, we group four catalysts differing in associated cation; in column 2, five anions differing in identity of the central atom; and in column 3, photocatalysts differing in the number of tungsten atoms in the anionic array and, hence, in size.

Because of the importance of catalyst solubility for effective photocatalysis and because the anions are substantially more stable in organic solvents than in aqueous solutions, we examined the effect of the associated cation of the heteropolyoxoanion solubility. Solvent compatibility for the sodium, ammonium, and tetrapropylammonium salts of **1** is listed in Table II. Association with the bulk tetraalkylammonium ion allows for effective solubilization of the heteropolyoxometalate in acetonitrile, dimethylformamide, and dimethyl sulfoxide, three polar aprotic solvents compatible with a wide array of organic functional groups.

Solvent dependence of the ultraviolet absorption maximum of the reference anion **1** is shown in Table III. The observed small solvent shifts are consistent with the assignment of the long-wavelength band to an oxygen-to-metal charge-transfer transition. This assignment correctly predicts oxidative photocatalytic behavior in the presence of potential donors. The observed spectral shift associated with pH changes may also be caused by structural change, dimerization having been suggested as important under highly basic conditions.[26] The significant broadening of the long-wavelength absorption tail is medium dependent,[11] as might be expected for charge-transfer transitions within a donor–acceptor complex.

Table IV. Absorption Maxima for Several Heteropolyoxoanions

HPA	solvent	λ_{max},[a] nm
$Na_3PW_{12}O_{40}$	H_2O	255
$(NH_4)_3PW_{12}O_{40}$	H_2O	255 (261, 249, 245)
$(Pr_4N)_3PW_{12}O_{40}$	CH_3CN	263
$(NH_4)_3PW_{12}O_{40}$	DMF	267
$H_3PW_{12}O_{40}$	H_2O	258
$Na_6H_2W_{12}O_{40}$	H_2O	262
$H_5FeW_{12}O_{40}$	H_2O	218, 303
$H_4SiW_{12}O_{40}$	H_2O	263
$HK_5CoW_{12}O_{40}$	H_2O	263, 625
$HK_5CoW_{12}O_{40}$	CH_3CN	256 (670, 650, 613, 575)
$(NH_4)_6P_2W_{18}O_{62}$	H_2O	257, 309
$(NH_4)_{14}P_5W_{30}O_{110}$	H_2O	256, 309
$(Bu_4N)_4H_3SiW_9V_3O_{40}$	CH_3CN	250, 260, 373, 500
$(Bu_4N)_5H_4P_2W_{15}V_3O_{62}$	CH_3CN	236

[a] ±2 nm.

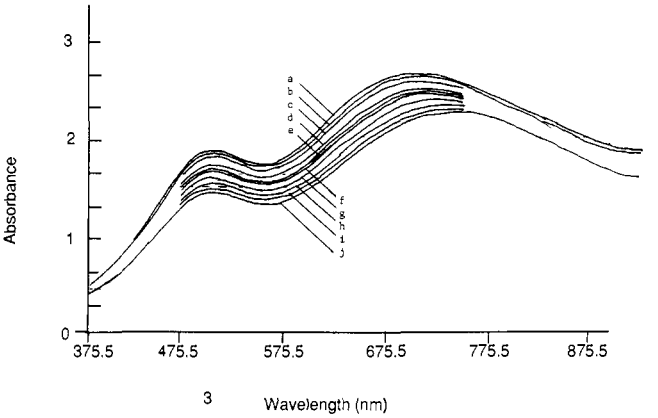

Figure 1. Recovery of **1** by thermal oxidation of its doubly reduced salt formed by photocatalytic oxidation of alcohol: absorption spectra at 30-s intervals (a–j) after exposure of exhaustively reduced **1** to air.

Absorption maxima are listed in Table IV for other soluble members of the series. These tungstates possess, in general, a strong transition at about 260 nm. If an additional transition-metal atom is present, additional bands in the visible or long-wavelength ultraviolet regions are evident. The ammonium salts of phosphorus-centered tungsten aggregates ($(NH_4)_6P_2W_{18}O_{62}$ and $(NH_4)_{14}P_5W_{30}O_{110}$) also exhibit an additional band at 309 nm.

Upon 1:1 stoichiometric reduction of **1** with metallic zinc, two new bands characteristic of the reduced tungsten appear in the visible at 491 and at about 690 nm. The long-wavelength absorption band is insensitive to the identity of the central atom, suggesting that the added electron is associated with the tungstate framework and is not localized at the center of the complex anion. Similar features are observed in the one- or two-electron-reduced species spectrum, although a difference in extinction coefficient does differentiate the species. In fact, spectra of successively reduced (three or four electrons per **1**) tungstates in general appear to show only small blue shifts upon further reduction,[10,27] and the assignment of the level of catalyst reduction must be derived by back-titration with oxidizing agents.

That oxygen can function as such an oxidant can be seen in Figure 1, which shows absorption spectral evidence for spectral bleaching of the band that appears upon reduction (the regen-

(17) For example, see: Barrows, J. N.; Jameson, G. B.; Pope, M. T. *J. Am. Chem. Soc.* **1985**, *107*, 1771.
(18) Unoura, K.; Tanaka, N. *Inorg. Chem.* **1983**, *22*, 2963.
(19) Wu, H. *J. Biol. Chem.* **1920**, *43*, 180.
(20) North, E. O. *Inorganic Synthesis*; McGraw-Hill: New York, 1939; Vol. 1, p 129.
(21) Pope, M. T.; Baker, L. C. W. *J. Am. Chem. Soc.* **1960**, *82*, 1771.
(22) Booth, H. S. *Inorganic Synthesis*; McGraw-Hill: New York, 1939; p 1249.
(23) Mair, J. A. *J. Chem. Soc.* **1950**, 2364.
(24) Brown, D. H. *Spectrochim. Acta* **1963**, *19*, 1683.
(25) Baker, L. C. W.; McCutcheon, T. P. *J. Am. Chem. Soc.* **1956**, *78*, 4503.
(26) (a) Finke, R. G.; Droege, M. W. *J. Am. Chem. Soc.* **1984**, *106*, 7274. (b) The reported maxima do not change with time. Thus if any structural reorganization occurs, it occurs as soon as the anion is dissolved. The maxima thus correspond to the active photocatalyst, whether or not it is the crystalline **1**.
(27) Fruchart, J. M.; Herve, G.; Launay, J. P.; Massart, R. *J. Inorg. Nucl. Chem.* **1976**, *38*, 1627.

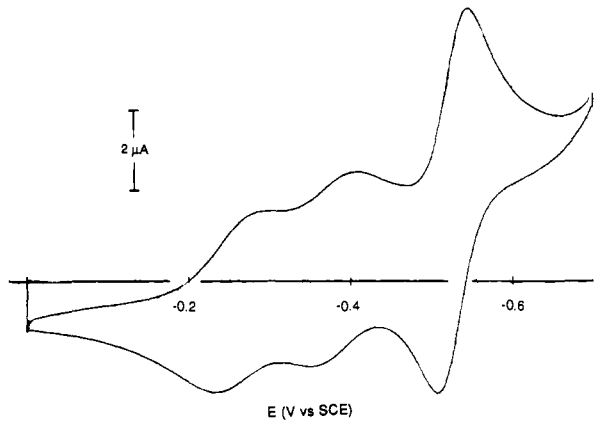

Figure 2. Cyclic voltammogram of **1** in water:dioxane (electrolyte = 1 M H_2SO_4, scan rate = 100 mV/s, 24 °C).

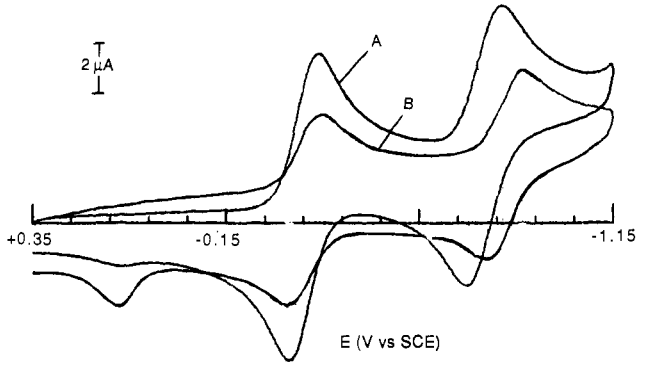

Figure 3. Cyclic voltammogram of **1** in acetonitrile (electrolyte = 0.1 M TBAP, scan rate = 100 mV/s, 24 °C). (A) $Na_3PW_{12}O_{40}$; (B) $(Pr_4N)_3PW_{12}O_{40}$.

eration of **1** from the doubly reduced salt) after exposure for varying periods to dissolved oxygen. Nearly complete recovery of the original spectrum is observed after sufficient time. This recovery is accompanied by a total disappearance of the intense blue color indicative of catalyst reduction.

A typical cyclic voltammogram of **1** in 1:1 water/dioxane is shown in Figure 2. The wave shape and peak separation indicate high reversibility, with two one-electron reductions followed by a two-electron reduction. This behavior mirrors that reported by Pope and Varga for the aqueous electrochemistry of several dodecatungstates.[28] When the solvent for the electrolysis is changed to acetonitrile, however, the two one-electron waves at −0.27 and −0.44 V (vs. SCE) fuse into a single two-electron wave shifted to −0.41 V (Figure 3), which is characterized by essentially the same peak height as the second two-electron wave and by a clear cathodic shift of the peak position. Clearly, environmental effects can shift the disproportionation equilibria in the polyoxoanions so that conditions can be devised for effective one- or two-electron exchanges. Parallel effects are observed in other members of the series, and peak potentials are summarized in Table V. Inclusion of silicon or vanadium in the heteropolyoxoanion caused a significant positive shift of the first reduction wave. In anions containing cobalt, an additional metal-based oxidation could be observed.

Bulk electrolysis of **1** showed that as many as four electrons can be added reversibly to the sodium salt in aqueous electrolytes. Coulometry also showed that the tetraalkylammonium salt can take up reversibly two electrons at −0.65 V (vs. SCE) and an additional two electrons when the potential is maintained at −1.15 V.

Photooxidations Initiated by Irradiation of Polyoxoanions

Heteropolytungstates and -molybdates can be used as photocatalysts for the oxidation of many water-soluble, hydroxylated organic compounds[1-11] and are even effective at water splitting,[3,10] although mechanistic details regarding the routes of activation remain obscure. Papaconstantinou and co-workers have shown that the photoreactivity of a series of dodecatungstates parallels their reduction potentials, although the oxidative susceptibility of a series of hydroxylated organic substrates did not parallel their oxidation potentials.[4] Large concentrations of simple alcohols were required for efficient photoreactivity, an observation suggestive of a very short-lived reactive excited state. They suggest a mechanism for the oxidation in which a diffusive encounter between the alcohol and the heteropolytungstate excited state induces hydrogen abstraction. A second photoactivation of the ketyl/reduced tungstate then produces the observed products.[1] Photophysical characterization of the excited state has not been accomplished since emission in the photoactive tungstates is weak, and the family has been claimed to be nonfluorescent.[1,11]

We find that methanol, 2-propanol, 2-butanol, cyclobutanol, and benzhydrol are cleanly oxidized to the corresponding carbonyls upon steady-state photoexcitation[14] of $Na_3PW_{12}O_{40}$ (**1**) in water (pH 1) or of $(n\text{-}Pr_4N)_3PW_{12}O_{40}$ (**2**) in acetonitrile (eq 1). The

$$RR'CHOH \xrightarrow{1^* \text{ or } 2^*} RR'C{=}O \qquad (1)$$

a, R = R′ = H
b, R = Et, R′ = H
c, R = Me, R′ = Et
d, R = R′ = $(CH_2)_3$
e, R = R′ = Ph

Table V. Half-Wave Potentials for the Electroreduction of Some Heteropolyoxoanions

elec-trode	compd	half-wave potential V vs SCE (peak to peak)
Pt[a,b]	$Na_3PW_{12}O_{40}$	−0.36 (90), −0.83[f] (140)
	$(Pr_4N)_3PW_{12}O_{40}$	−0.35 (90), −0.86[f] (90)
	$H_3PW_{12}O_{40}$	−0.05 (200), −0.28,[e] −0.81 (90)
	$H_4SiW_{12}O_{40}$	+0.13 (160), −0.87[f] (350)
	$H_5FeW_{12}O_{40}$	−0.17,[e] −0.37[e,f]
	$K_5HCoW_{12}O_{40}$	+1.13 (170), −0.42 (370), −0.80 (60)
	$(NH_4)_6P_2W_{18}O_{62}$	−0.27,[e] −0.60,[e] −0.80[e]
	$(NH_4)_{14}P_5W_{30}O_{110}$	−0.33,[e] −0.55,[e] −0.77,[e] −0.98[e]
	$(Bu_4N)_4H_3SiW_9V_3O_{40}$	+0.17 (150)[f]
	$(Bu_4N)_5H_4P_2W_{15}V_3O_{62}$	+0.27 (70), 0.00 (100)[f]
GC[a,b]	$Na_3PW_{12}O_{40}$	−0.25 (60), −0.45[d] (60), −0.63 (70), −0.88[e]
	$H_3PW_{12}O_{40}$	−0.25 (60), −0.44[d] (80), −0.53 (110), −1.00
	$(Pr_4N)_3PW_{12}O_{40}$	−0.24 (80), −0.75 (60)[f]
GC[a,c]	$H_3PW_{12}O_{40}$	−0.25 (60),[d] −0.38 (60),[d] −0.53 (60)[d]
	$Na_3PW_{12}O_{40}$	−0.27 (60), −0.44 (70), −0.58 (60)

[a] Reported values are referenced to SCE Measurements were made against $Ag/AgNO_3$ on a Pt disk and against SCE on glassy carbon (GC) electrodes. [b] In acetonitrile with tetrabutylammonium perchlorate (TBAP, 0.1 M) as supporting electrolyte; scan rate = 100 mV/s. [c] In a 1:1 water–dioxane containing 0.36 M H_2SO_4 as supporting electrolyte. [d] Peaks are trailing waves. [e] Poor reversibility. [f] Other peaks were obscured by the solvent window.

Table VI. Photocatalyzed Oxidation of Alcohols by **1**: Product Characterization and Quantum Yields

alcohol	product	$\Phi_{obsd} \pm 0.01$ ($\times 10^2$)
methanol	formaldehyde	0.29
1-propyl	1-propanone	1.44
sec-butyl	2-butanone	1.08
cyclobutyl	cyclobutanone	1.20
tert-butyl	acetone, formaldehyde	<0.01

Table VII. Photocatalyzed Oxidation of Benzylic CH by **1**: Product Characterization and Relative Quantum Yields

alcohol	product	$\Phi_{rel} \pm 0.1$
benzhydrol	benzophenone	2.5
toluene	benzaldehyde, benzyl alcohol	<0.1
benzyl methyl ether	methyl benzoate	1.0
diphenylmethane	benzophenone	4.5

(28) Pope, M. T.; Varga, G. M., Jr. *Inorg. Chem.* **1966**, *5*, 1249.

Table VIII. Relative Rates for the Photocatalyzed Oxidation of Benzhydrol by Several Heteropolyoxoanions[a]

photocatalyst	rates of oxidation[b]
$WO_2(OR)_2$[c]	60
$(Bu_4N)_4H_3SiW_9V_3O_{40}$	<1
$Na_3PW_{12}O_{40}$	100
$K_5HCoW_{12}O_{40}$	<1
$H_5(FeW_{12}O_{40})$[d]	346
$Na_6H_2W_{12}O_{40}$[d]	732
$K_4SiW_{12}O_{40}$	<1
$H_4SiW_{12}O_{40}$	<1
$(Bu_4N)_5H_4P_2W_{15}V_3O_{62}$	<1
$(NH_4)_6P_2W_{18}O_{62}$	<1
$(NH_4)_{14}NaP_5W_{30}O_{110}$	<1
$(WO_3)_n$[d]	45
WO_3/Pt[d]	~100

[a] All samples were irradiated with 300-nm low-pressure Hg lamps for approximately 20 h in a CH_3CN-H_2O (70:30) solvent mixture. [b] Relatives rates of oxidation were monitored by the appearance of the benzophenone signal in the HPLC. Error limit ±1, except for the $H_5FeW_{12}O_{40}$ and $Na_6H_2W_{12}O_{40}$ species (±35). [c] The alcohol substrate is covalently attached in the tungstate ester; it is only absorbed in other members of the series. [d] The soluble heteropolytungstate solutions were light opaque. Those of $H_5(FeW_{12}O_{40})$, $Na_6H_2W_{12}O_{40}$, WO_3, and WO_3/Pt were heterogeneous: thus, light absorption cannot be quantitatively equated. The reported value represents relative rates for appearance of oxidation products under constant illumination. Platinum coverages in the range of 1–5 wt % gave comparable rates (±20%).

chemical identity of the isolated oxidation products and quantum yields for their formation are listed in Table VI. A chemically parallel photooxidation is also observed if a solution of $WO_2(OR)_2$ or a suspension of platinized powdered WO_3 in alcoholic acetonitrile is similarly irradiated. The blue color characteristic of catalyst reduction is also formed upon irradiation in the presence of tertiary alcohols, although simple carbonyl products are not found (see below). Compounds lacking polar functionality but containing oxidizable benzylic CH bonds were also oxidized by the excited polyoxoanion (Table VII).

The effect of the substrate structure on the quantum yield for the production of reduced catalyst can be seen in the data in Table VI. Compounds having sterically accessible polar functionality were efficiently oxidized. The efficiency of the oxidation was governed by the oxidation potential of the alcohol, the avability of α-hydrogens, and the tightness of the association with the photocatalyst: primary alcohols > secondary alcohols > methanol ≫ tertiary alcohols > aryl methyl.

The effect of photocatalyst structure on the relative rates of oxidation in the photocatalyzed oxidation of benzhydrol is shown in Table VIII. Replacing surface-accessible tungsten atoms with vanadium or the central atom with silicon significantly reduced the observed photoactivity, while platinization of the heterogeneously dispersed WO_3 particles improved the rate of photocatalyzed oxidation somewhat. Ammonium salts of the higher tungstate aggregates showed nearly no photoactivity.

Complexation with Alcohol

Several types of spectroscopic evidence suggest strong precomplexation of the alcohol and the photocatalyst. The ultraviolet absorption maxima of the sodium and tetrabutylammonium salts of **1** in several polar organic solvents were red-shifted (3–10 nm) in organic solvents by the addition of water or alcohol, consistent with the assignment discussed earlier for the primary electronic transition as a ligand-to-metal charge-transfer band. NMR studies reveal multiplicity changes consistent with complexation in the spectrum of 1-propanol in acetonitrile-d_6 upon addition of **1** (Figure 4). In the absence of the catalyst, 1-propanol in CD_3CN shows the hydroxyl resonance as a triplet at δ 2.8 and a quartet (δ 3.5) for the adjacent methylene group. Upon addition of the heteropolytungstate, the hydroxyl resonance sharpens to a singlet, and the multiplicity of the methylene simplifies to a triplet. Such changes require rapid proton exchange at the catalyst surface, covalent bonding as a surface tungstate, or strong hydrogen bonding at an oxide site at the surface of **2**.

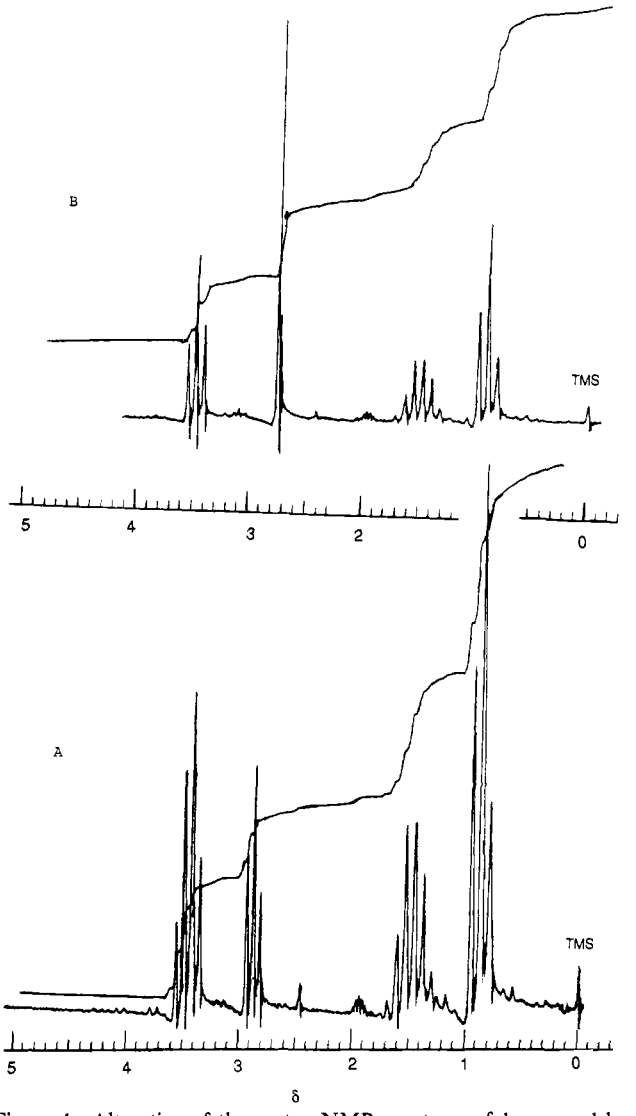

Figure 4. Alteration of the proton NMR spectrum of 1-propanol by addition of small quantities of **1**: (A) 1-propanol in CD_3CN; (B) same spectrum, saturated with **1**.

Hill has recently reported the X-ray structure of a preassociation complex between tetramethylurea (TMU) and $H_3PMo_{12}O_{40}$, the molybdate structurally analogous to our tungstate.[29] In that structure the shortest (TMU–polyoxoanion) nonbonded distance was found to be the 2.894-Å separation between the electron-rich urea oxygen and the (apparently) electron-deficient molybdenum-bound (terminal oxygen). This latter oxygen is presumably rendered electron deficient by virtue of back-bonding contributions $(^-O_4)^-Mo{\equiv}O^+$. If parallel electronic structure is encountered in the tungstates, precomplexation with electron-rich alcohol functionality is certainly reasonable.

That alcohol precomplexation does occur can be established by examining fluorescence lifetimes and by flash excitation of potentially precomplexed substrates. In contrast to previous studies, we were able to observe weak fluorescence from highly purified sodium and tetrapropylammonium salts of **1**. The fluorescence lifetimes of these salts in water and acetonitrile were determined via single-photon-counting techniques to be 1.5 ± 0.5 and 1.6 ± 0.5 ns, respectively. The observed fluorescence was completely quenched by even very small quantities (10^{-3} M) of added alcohol. From the detection limits of our single-photon-counting instrumentation, this result requires a quenched lifetime shorter than 0.5 ns. From the usual kinetic expression for bi-

(29) Hill, C. L.; Renneke, R. F.; Williamson, M. M. *Chem. Commun.* **1986**, 1747.

Scheme I. Proposed Mechanism for the Photocatalyzed Oxidation of 2-Butanol by **1***[a]

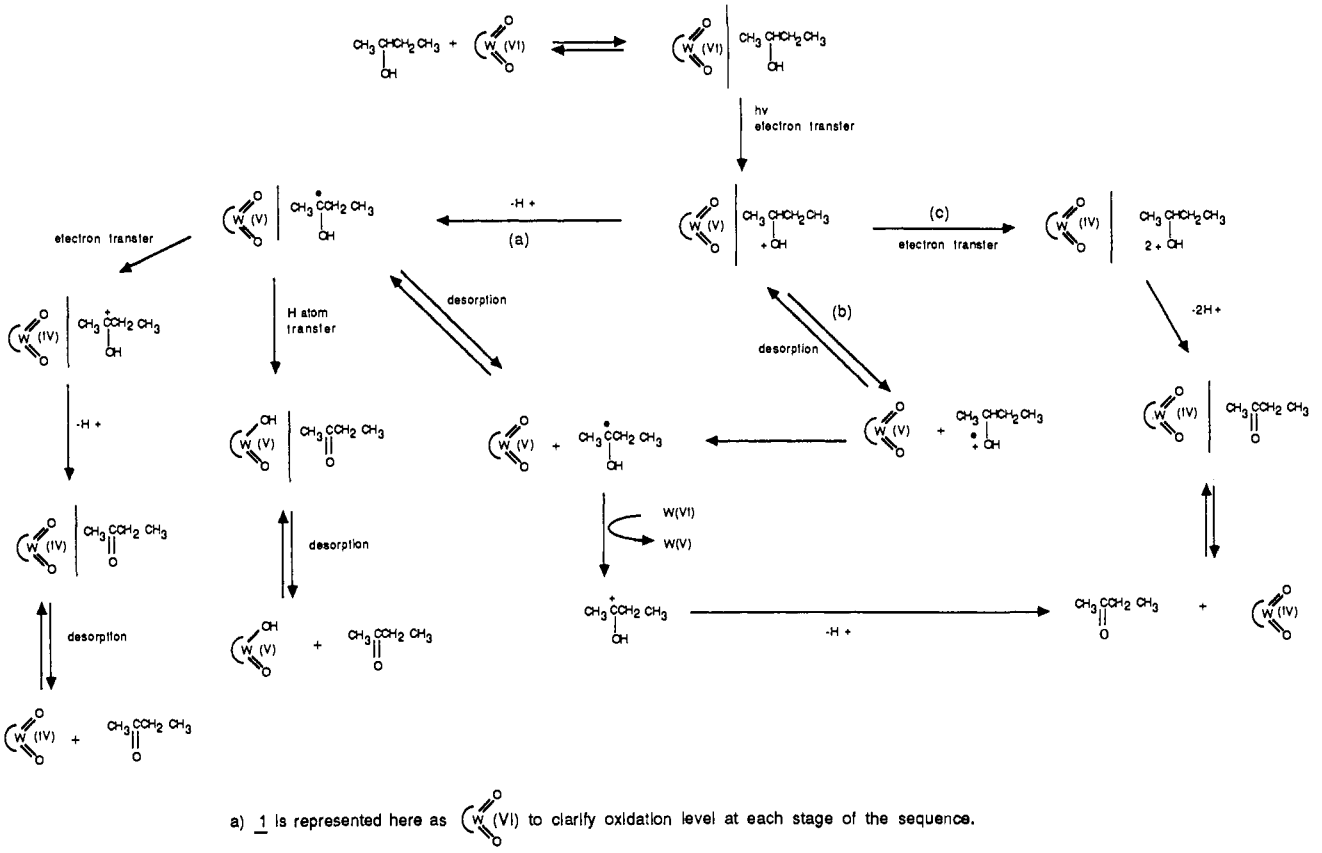

a) 1 is represented here as W(VI) to clarify oxidation level at each stage of the sequence.

molecular quenching ($1/\tau_{obsd} = 1/\tau_0 + kq[Q]$), this requires a bimolecular rate constant greater than 1.3×10^{12}. Since the diffusion-limited rate in water at room temperature is 10^{10},[30] the kinetic quenching occurs at a rate about 2 orders of magnitude faster than unactivated diffusional encounter. This can only be attained by preassociation of the quencher (i.e., the alcohol) with the photocatalyst. This kinetic conclusion is thus in full accord with Hill's recent structural characterization of a preassociation complex and with Pope's previous demonstration[31] from NMR spectroscopy.

Flash excitation[32] of a deoxygenated solution of benzhydrol (4×10^{-3} M) in acetonitrile gave rise to an observed emission (λ = 410 nm, $\tau = 6.2 \pm 0.5$ ns) assigned to the lowest singlet excited state, followed by a formation of a longer lived transient (λ = 420 nm, $\tau = 1.0 \pm 0.5$ μs) assigned to the benzhydrol triplet with a rise time equal to the singlet fluorescence decay. The addition of small concentrations (10^{-4} M) of **1** completely quenched both the singlet and triplet states. In no case could transient formation of benzhydrol ketyl, a radical whose transient behavior is well-known,[33] be detected. These species would be observed if the primary photoprocess involved either hydrogen abstraction or a one-electron exchange followed by deprotonation. That such preassociation equilibria would be favored for sterically unencumbered alcohols may provide a reasonable explanation for the parallel previously reported chemoselective photooxidation of primary alcohols on TiO_2 suspensions.[34]

Some of the relative inefficiency in the photocatalyzed benzylic oxidations can be ascribed to poor preequilibrium complexation (the substrates lacking polar groups), and hence to less efficient electron exchange upon photoactivation. The requirement for precomplexation can also help to explain the lack of photoactivity in polyoxoanions modified by surface vanadation. When V^{5+} is substituted for W^{6+}, as in $(Bu_4N)_4H_3SiW_8V_3O_{40}$ or $(Bu_4N)_5H_4P_2W_{15}V_3O_{62}$, the complex will bear three extra negative charges so that electron density shifts toward the vanadium oxide terminal oxygen ($-O_4V{\equiv}O^-$) so that the oppositely charged terminal oxygens will interfere electrostatically with the necessary complexation at VO sites. Since negative charge is delocalized in the polyoxoanions by cooperative trans effects,[14] the tungsten sites should also exhibit diminished activity. Thus, no photoactivity is observed despite the more favorable redox potential reported in Table V.

Proposed Mechanism for the Photocatalyzed Alcohol Oxidation

The above observations lead us to propose the mechanism for photocatalyzed oxidation of alcohols on irradiated heteropolyoxotungstates shown in Scheme I. In contrast to Papaconstantinou's preliminary suggestions for the photoreaction of *1* in water or in neat alcohol, we find in acetonitrile or in aqueous alcohol that precomplexation of the alcohol with the heteropolyoxotungstate must precede photoactivation, much as preadsorption at the solid–liquid interface is required for semiconductor-mediated photoelectrochemical effects. Photoexcitation of the photocatalyst:alcohol complex then generates an excited state in which electron transfer from the adsorbed alcohol to the tungstate produces a reduced metal (W(V)) complexed to the oxidized alcohol. Three fates are available to such a complex: it can deprotonate to form a surface-bound radical (path a), it can desorb to produce a solvated alcohol cation radical (path b), or it can be further oxidized on the catalyst surface (path c).

If path a is followed, the radical complex likewise has three parallel fates: further electron transfer within the complex can generate W(IV) and the protonated carbonyl, an energetically favorable process as judged by the relative redox potentials of the second reduction of **1** and those of typical α-hydroxy radicals;

(30) Bamford, C. H.; Tipper, C. F. H. *Compr. Chem. Kinet.* **1977**, *8*, 114.
(31) Barcza, L.; Pope, M. T. *J. Phys. Chem.* **1975**, *79*, 92.
(32) Transient spectroscopic measurements were conducted with the fourth harmonic of a mode-locked Nd-YAG laser. Time-resolved transient spectra were obtained on a previously described apparatus at the Center for Fast Kinetics Research at The University of Texas: Lindig, B. A.; Rodgers, M. A. J. *J. Phys. Chem.* **1979**, *83*, 1683.
(33) Simon, J. D.; Peters, K. S. *J. Am. Chem. Soc.* **1981**, *103*, 6403.
(34) Hussein, F. H.; Pattenden, G.; Rudham, R.; Russell, J. J. *Tetrahedron Lett.* **1984**, *25*, 3363.

Scheme II. One- vs Two-Electron Oxidation of Cyclobutanol

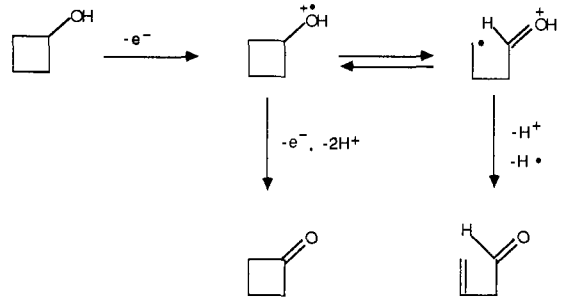

hydrogen atom transfer will generate the protonated doubly reduced heteropolyoxoanion and the adsorbed ketone; or desorption of the radical gives a free species that will require a second oxidative encounter with excited **1** to produce observed product.

Distinction between the first two options available after deprotonation is difficult. The cyclic voltammetry studies discussed earlier affirm the much easier removal of the second electron than the first from **1** under appropriate circumstances. Furthermore, previous investigation has shown that the relative oxidizability of the substrate is loosely related to the relative efficiency of the photocatalyzed conversion. The ordering of quantum yields for the alcohols shown in Table VI parallels that of substrate ionization potential, if corrected for the number of α-hydrogens and hence for steric accessibility of the catalyst surface (higher quantum efficiency for the more ionizable alcohol: secondary > primary > methanol). These observations are ambiguous, however, for α C–H bond strengths follow the same ordering. Previous reports of substantial isotope effects (k_H/k_D = 3.7 for isopropyl-d_2 alcohol)[5] may be more consistent with the loss of hydrogen as an atom than as a proton, but not convincingly so.[35] Thus, either of the two routes emanating from the adsorbed radical, both of which involve the loss of two protons and two electrons before desorption, seem reasonable.

Desorption of the free radical and diffusive encounter with a second excited state, however, is rendered unlikely by our failure to detect the stabilized benzhydrol radical in flash experiments and by the observation of kinetics inconsistent with a second diffusive encounter. Thus, if path a is followed, loss of two electrons and two protons from the substrate is likely before desorption of the substrate from the irradiated catalyst surface.

If path b were followed, the alcohol radical cation would be expected to rapidly deprotonate in acetonitrile or in the modest pH aqueous solutions employed here. This deprotonation would produce the same radical discussed earlier as being formed by desorption from the complex formed in path a, and its involvement suffers the same mechanistic problems.

The operation of path c requires the endothermic oxidation of the alcohol cation radical within the photogenerated pair to be kinetically competitive with deprotonation. Although absolute rates are known for neither route, this possibility seems unlikely, especially in acetonitrile or at neutral pH, since alcohol radical cations are known to have highly negative pK values. Intact desorption of a dicationic species from a metal oxide surface is also unprecedented.

We therefore prefer the two-electron, two-proton route to path a and sought to verify this prediction by examining the course of two alcohol photooxidations in which different products would ultimately be observed from one- and two-electron routes. Cyclobutanol is a sensitive probe, for it has been established that single-electron oxidation selectively produces open-chain products (Scheme II), whereas two-electron oxidation will yield cyclobutanone.[36] Our observation of cyclobutanone as the sole isolable product in the photocatalyzed oxidation mediated by **1** supports the importance of two-electron routes preceding desorption of the oxidized substrate. Independent work by Miwa and co-workers[37] has pointed out such phenomena.

Our preferred mechanism requires removal of the α-hydrogen from the alcohol, either as a proton or a hydrogen atom, before desorption. To test this requirement *tert*-butyl alcohol, which lacks this structural feature, was examined as a substrate for the oxidation. We find that this species serves as a much less efficient donor toward the excited state of **1**, its relative rate being about 2 orders of magnitude lower than that of primary or secondary alcohols (Table VI). Cleavage products were observed, however, upon prolonged irradiation. The traces of acetone and formaldehyde observed allow us to implicate the intermediacy of an oxidized radical, although the stage at which it desorbs from the photocatalyst is unclear. The reduced reactivity can be accommodated in our mechanism either as a steric interference with precomplexation or as a kinetic retardation of the bond cleavage of a C–C vs a C–H bond in the adsorbed radical cation.

Photocatalyst Structure

There is striking variation in the efficiency of photocatalyzed oxidation by tungstates of varying molecular complexity (Table VIII). We consider the observed trends according to the groupings of Table I. First, although solubility differences among the salts listed in column 1 of Table I made comparison of photoreactivity in the same medium impossible, comparable activities (within a factor of 2) were observed for $H_3PW_{12}O_{40}$, $Na_3PW_{12}O_{40}$, and $(Pr_4N)_3PW_{12}O_{40}$, suggesting that electronic properties were not significantly influenced by the identity of the associated cation. The ammonium salt $(H_4N)_3PW_{12}O_{40}$ was insufficiently soluble in any medium to test for homogeneous photoactivity. The photochemistry in the series seems to be most easily understood as involving the excited state of a surface-localized W≡O multiple bond precomplexed with a redox partner.

Greater activity was observed upon changing the central atom to H or Fe from P, but nearly no activity could be observed with Si or Co as the central atom. Since these latter two anions also exhibit anomalous reduction potentials, we suspect that the diminished photoactivity has an a electronic basis that allows for more efficient back electron transfer to the adsorbed oxidized species. That iron and cobalt have opposite effects on photoactivity makes it unlikely that analogy can be drawn between the identity of the central atom of heteropolyoxoanions and n or p doping of semiconductor photocatalysts.

The differences in relative rate along the series $WO_2(OR)_2$, **1**, WO_3, and WO_3/Pt were modest. Thus, the efficiency seems to be related more closely to the oxidation level of tungsten (which is constant thoughout the series) and to the existence of surface sites for effective substrate adsorption than to developing colligative properties in the series. The observed improvement in oxidative photoefficiency upon platinizing suspended WO_3 powders is consistent with enhanced charge separation at the semiconductor–solution interface, which has been reported previously for other metal oxides.[16] It should be noted that comparable oxidation rates for alcohols were observed when the alcohol was adsorbed onto the photoactive substrate and when it was covalently attached as a tungstate ester, implying similar strong adsorption with either catalyst.

Aggregates of **1** (e.g., $(NBu_4)_5H_4P_2W_{15}V_3O_{62}$, $(NH_4)_6P_2W_{18},3_{62}$, and $(NH_4)_{14}NaP_5W_{30}O_{110}$) showed nearly no photoactivity. In contrast to **1**, these aggregates show poor electrochemical reversibility. Thus, these aggregates lack both the localized 1:1 interaction of adsorbate to heteropolytungstate of the simple photocatalysts and a sufficient size for the development of a full space-charge region as is encountered on an irradiated semiconductor particle. The ammonium salts also exhibit an additional adsorption band at 309 nm, suggesting the accessibility of an additional low-lying excited state that cannot induce reduction, yet can provide a nonradiative pathway for degradation of the oxygen-to-metal charge-transfer excitation. For the reasons discussed earlier, we predict that high photoactivity should be

(35) Yamase, T.; Watanabe, R. *J. Chem. Soc., Dalton Trans.* **1986**, 1669.
(36) Meyer, K.; Rocek, J. *J. Am. Chem. Soc.* **1972**, *94*, 1209.
(37) Nomiya, K.; Miyazaki, T.; Maeda, K.; Miwa, M. *Inorg. Chim. Acta* **1987**, *127*, 65.

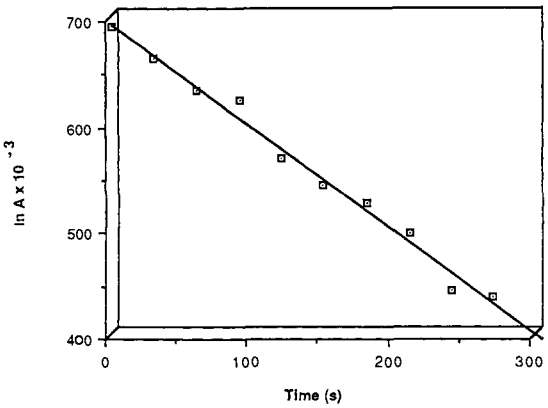

Figure 5. Kinetic profile for photocatalyst regeneration.

encountered in polyoxoanions bearing substantial positive charge at their terminal oxygen atoms and hope to test this prediction in future work.

Catalyst Regeneration

Since the utility of these photocatalysts will depend on their long-term stability, it is important to establish both the extent and the rate of recovery of the photocatalyst. In our preparative experiments, we have established that at least a 1000-fold ratio of product to photosensitizer can be attained with **1** or **2** in the presence of oxygen. This turnover number (>1000) thus implies less than 0.1% decomposition of photocatalyst per cycle. This is consistent with our earlier observation of nearly complete recovery of the catalyst from spectral evidence (Figure 1). Since the heteropolyoxoanion photocatalysis described herein is photomediated (requiring a photon for each cycle, rather than a process involving photogeneration of a reactive species that initiates a product-amplifying chain), the turnover rate is light-intensity dependent. The low observed quantum efficiencies for photocatalyzed oxidation will ultimately be the major limitations of these materials.

In a previous study, Ward and co-workers reported that photocatalytic oxidative activity of heteropolymolybdates was higher at the beginning of the reaction, decreasing to a steady state as the reaction proceeded.[5] A reasonable interpretation of this observation is that reduced species formed upon photoreduction are less active and compete for photons with the more active catalyst present initially. We sought therefore to characterize the kinetics of catalyst regeneration by oxygen and to determine whether other reagents might be identified that could more efficiently regenerate the active photocatalyst. In Figure 5 is plotted the rate of regeneration of **1** in air-saturated solution. The linearity of the plot indicates that either a single reduced species interacts with oxygen or that nearly identical rate constants are observed in the reaction of oxygen with more than one reduced material. Since the extinction coefficient calculated for a sample of **1** exhaustively photoreduced under nitrogen shows the presence of both two- and four-electron-reduced species, the latter option must be correct. Using the known solubility of oxygen in acetonitrile, one can calculate a pseudounimolecular rate constant for the reoxidation: 3.7×10^{-2} s^{-1}. Addition of 0.01 M maleic anhydride produces a much more rapid bleaching of the tungstate blue, and a more complete description of its reactivity allows for a sacrificial reduction of organic substrates to be driven by irradiation of heteropolyoxoanions in alcoholic solution.

These photocatalysts may offer signifiant advantage, however, in allowing for substrate activation under less rigorous environments. The course and chemical yields for oxidation of methanol and primary alcohols are quite similar with these catalysts whether thermal[38] or photochemical activation is employed, but the course of other substrates may indeed differ significantly. Thermal activation of molybdate polyanions, for example, gives only dehydration of *tert*-butyl alcohol, whereas our photochemical activation with tungstate heteropolyoxoanions gave skeletal cleavage.

Summary

Thus, photocatalytic reactivity on heteropolyoxoanions is expected to be governed by preadsorption equilibria and by the catalyst's excited-state reducibility. Two-electron, two-proton exchange occurs before the oxidation product desorbs from the catalyst surface. Structural complexity of the photocatalyst can significantly influence the efficiency of the photoinduced electron transfer. High turnover numbers imply that oxygen can regenerate the reduced catalyst with high chemical efficiency. Relatively low quantum yields are observed in these photon-driven conversions. Such effects, somewhat similar to those suggested by Ward and co-workers from steady-state measurements on heteropolymolybdates,[10] can explain the trends observed earlier for the relative photoreactivities of several heteropolyoxotungstates.

Experimental Section

General Procedures and Instrumentation. Commercial (Aldrich and Fisher) samples of methanol, 2-butanol, 1-propanol, and cyclobutanol were distilled to >99% gas chromatographic purity. Solvents employed were reagent grade. Tetrahydrofuran (THF) and ether were distilled under a nitrogen stream from potassium metal or lithium aluminum hydride. Acetonitrile used for steady-state irradiations and bulk electrolysis was HPLC grade used without further purification. Acetonitrile used as a solvent for analytical electrochemical measurements was HPLC grade, distilled immediately before use from CaH_2.

High-pressure liquid chromatography (HPLC) was conducted with a Waters Associates, μBondapak C-18 P/N 27324 S/N analytical column using a Model 440 absorbance detector with a 280-nm filter or a R401 differential refractometer. Cyclic voltammograms were obtained either with a Bioanalytical Systems (BAS 100) electrochemical analyzer or with a Princeton Applied Research system composed of a universal programmer (Model 175), a potentiostat/galvanostat (Model 173), a digital coulometer (Model 179), and a Houston Instruments Model 2000 *x–y* recorder. Ultraviolet and visible absorption spectra (UV-vis) were obtained on either a Cary 15 or 17 or a Hewlett-Packard 8451 diode-array spectrophotometer. Gas–liquid chromatography (GC) was accomplished with a Varian Aerograph 1400 chromatograph equipped with a capillary column (50 m, BP-1). Gas chromatography/mass spectroscopy (GC/MS) was performed on a Finnigan 4023 automated GC/MS with an INCOS data system. Low-resolution mass spectra were obtained on a DuPont 21-491 mass spectrometer. Nuclear magnetic resonance (NMR) spectra were obtained on a Varian EM-390, a Varian FT-80, or a Nicolet NMC-1280 spectrometer.

Irradiations were carried out with a cyclic array of low-pressure mercury arcs (blazed at 254, 300, or 350 nm) in a Rayonet reactor, with a quartz-filtered 450-W Hanovia medium-pressure mercury arc, or with a 1000-W xenon lamp. All photoreactions were conducted in quartz vessels.

Preparation of the Photocatalysts. The heteropolytungstates investigated here were prepared by previously described methods.[19–25,39–42] All salts were recrystallized before use and were dried in a vacuum desiccator (overnight). Platinization of WO_3 was conducted by a procedure parallel to that used by Bard and co-workers for platinization of TiO_2.[43] The samples employed had platinum coverages of 1–5 wt %.

Photooxidation of Alcohols in the Presence of Heteropolytungstates. In a typical run, 20 mL of a 2 M solution of the alcohol in either acetonitrile or water (pH between 1 and 5) was irradiated for approximately 20 h in the presence of 1×10^{-3} M photocatalyst either under a slow stream of oxygen or in a sealed ampule prepared at atmospheric pressure. Product identification was accomplished by direct analysis of the photolysate by GC or HPLC and by coinjection with authentic samples. After a standard workup (washing the reaction mixture with an equal volume of water and extracting twice with ether), isolable products were identified by NMR and GC/MS. Alternatively, hydrazone derivatives prepared by treatment of the photolysate with 2,4-dinitrophenylhydrazine were isolated and identified.[44]

(38) Cheng, W. H.; Chowdhry, U.; Ferretti, A.; Firment, L. E.; Groff, R. P.; Machiels, C. J.; McCarron, E. M.; Ohuchi, F.; Staley, R. H.; Sleight, A. W. *Heterogeneous Photocatalysis*; Shapiro, B. L., Ed.; Texas A&M Press: College Station, TX, 1984; p 165.

(39) Pope, M. T.; Baker, L. C. W. *J. Am. Chem. Soc.* **1960**, *82*, 4176.
(40) Zado, F. *J. Inorg. Nucl. Chem.* **1963**, *25*, 1115.
(41) Preyssler, C. *Bull. Soc. Chim. Fr.* **1970**, 30.
(42) Alizadeh, M. H.; Harmalker, S. P.; Jeannin, Y.; Martin-Frère, J.; Pope, M. T. *J. Am. Chem. Soc.* **1985**, *107*, 2662.
(43) Kraeutler, B.; Bard, A. J. *J. Am. Chem. Soc.* **1978**, *100*, 2239.
(44) Buckingham, D. *Q. Rev., Chem. Soc.* **1969**, *23*, 37.

Since benzhydrol absorbs light in the same wavelength region as the photocatalyst, special conditions were required to ensure exclusive excitation of the catalyst when this substrate was used. A dilute solution (6.5×10^{-4} M) of benzhydrol in a saturated solution of photocatalyst gave >99% light adsorption by the heteropolyoxotungstate. Similar concentration adjustments were also made with the benzylic substrates (Table VII). Products and relative rates of oxidation are listed in Tables VI and VIII.

Actinometry. Standard ferrioxalate actinometry methods were employed.[45] All manipulations were conducted in the dark or under a safety light. Pairs of light-opaque samples were irradiated in symmetrically placed vessels about the irradiation source for identical irradiation periods. Photocatalyst reduction was determined spectroscopically at 645 nm, and product yields were determined by GC or HPLC against an internal standard. An absolute measurement of the quantum efficiency of **1** was made, and all other measurements are reported relative to this absolute value.

Determination of the Extinction Coefficient of Reduced Heteropolytungstate. A dilute solution of **1** (2.0×10^{-4} M) or other heteropolytungstate was exhaustively irradiated under argon to a constant absorption at 690 nm. Identical absorption was attained by treatment under argon with excess zinc metal. Extinction coefficients were then calculated from the Beer-Lambert law.

Regeneration of the Photocatalyst. The exhaustively reduced solutions described above were opened to air and, while stirring, a UV-vis spectrum was recorded at 30-s intervals (Figure 1).

Electrochemistry. Cyclic voltammograms were recorded in a three-electrode cell[43] using a 1.2-mm platinum disk as the working electrode, a Pt foil flag or coil as the counter electrode, and a $Ag/AgNO_3$ reference. All compounds were analyzed as 1×10^{-3} M solutions with 0.1 M tetrabutylammonium perchlorate (TBAP) as electrolyte. Peak positions observed are listed in Table V.

Bulk electrolysis was carried out in a two-cell compartment similar to the analytical cell except that a mercury pool was employed as the working electrode. Under controlled potential, current flow was measured by digital coulometry.

NMR Complexation. A saturated solution of **1** in deuteriated acetonitrile was prepared. Two drops of alcohol were added and the spectrum was recorded. The comparison shown in Figure 4 was made with an identical concentration of alcohol in neat CD_3CN.

Acknowledgment. This work was supported by the Army Research Office. We happily acknowledge the technical assistance of Dr. Stephen Atherton of the Center for Fast Kinetics Research, a facility supported by the National Institutes of Health and by The University of Texas where the flash photolysis and single-photon-counting experiments were conducted. We are grateful to Professor Richard Finke, University of Oregon, for the samples of the vanadium-containing tungstates examined here and for extremely helpful discussions and suggestions.

(45) Hatchard, C. G.; Parker, C. A. *Proc. R. Soc. London, Ser. A* **1956**, *A235*, 518.
(46) Hardee, K. L.; Bard, A. J. *J. Electrochem. Soc.* **1977**, *124*, 215.

Complementarity and Chiral Recognition: Enantioselective Complexation of Bilirubin

David A. Lightner,* Jacek K. Gawroński, and W. M. Donald Wijekoon

Contribution from the Department of Chemistry, University of Nevada, Reno, Nevada 89557-0020. *Received April 27, 1987*

Abstract: Bichromophoric (4*Z*,15*Z*)-bilirubin-IXα, the cytotoxic pigment of jaundice, adopts either of two intramolecularly hydrogen-bonded enantiomeric conformations that are in dynamic equilibrium in solution. Added cinchona alkaloids, such as quinine, caused dichloromethane solutions of bilirubin to become intensely circular dichroic ($|\Delta\epsilon| \simeq 130$ L·mol^{-1}·cm^{-1}) in the region of the pigment's long-wavelength UV-visible absorption band (~450 nm). The optically active base acts as a chiral solvating agent to induce an asymmetric transformation of bilirubin, whose intense bisignate circular dichroism Cotton effect is characteristic of intramolecular exciton coupling.

(4*Z*,15*Z*)-Bilirubin-IXα (BR-IX), the yellow-orange, lipophilic, cytotoxic pigment of jaundice, is produced in abundant quantities in mammals by catabolism of heme and is transported as an association complex with albumin to the liver for glucoronidation and excretion.[1] The structure of the pigment has long been of interest owing to its importance in nature and its unusual solubility properties. Although the constitutional structural was proved over 40 years ago by classical methods,[2] its conformational structure was revealed only recently—by X-ray crystallography[3] and NMR spectroscopy.[4] Perhaps the most striking aspect of the three-dimensional structure of BR-IX is its ability and marked tendency to form extensive intramolecular hydrogen bonds, which link the polar carboxylic acid and lactam functionalities (Figure 1). This has important implications for biological function. It governs the shape and polarity of the molecule and explains the tremendous solubility differences between BR-IX and its constitutional isomers with propionic acid groups *not* located at C-8 and C-12. It also reveals the BR-IX structure as a potentially equilibrating pair of conformational enantiomers that interconvert by breaking and remaking all of its intramolecular hydrogen bonds. As such, BR-IX may be viewed as a racemic mixture (of A and B, Figure 1), whose crystals[3a] and solutions in isotropic solvents are optically inactive. However, in the presence of a chiral solvating agent, the bilirubin conformational enantiomers may act as chiral substrates (or templates) for molecular recognition.[5] For example, in the presence of cyclodextrins[6] or albumins,[7] BR-IX exhibits optical activity.[8]

(1) Lightner, D. A.; McDonagh, A. F. *Acc. Chem. Res.* **1984**, *17*, 417-424.
(2) (a) Fischer, H.; Plieninger, H.; Weisbarth, O. *Hoppe-Seyler's Z. Physiol. Chem.* **1941**, *268*, 197-226. (b) Fischer, H.; Plieninger, H. *Hoppe-Seyler's Z. Physiol. Chem.* **1942**, *274*, 231-260.
(3) (a) Bonnett, R.; Davies, J. E.; Hursthouse, M. B.; Sheldrick, G. M. *Proc. R. Soc. London, Ser. B.* **1978**, *202*, 249-268. (b) LeBas, G.; Allegret, A.; Mauguen, Y.; DeRango, C.; Bailly, M. *Acta Crystallogr., Sect. B.* **1980**, *B36* 3007-3011.
(4) For leading references, see: Kaplan, D.; Navon, G. *Isr. J. Chem.* **1983**, *23*, 177-186.
(5) For leading references, see: Rebek, J., Jr. *Science (Washington, D.C.)* **1987**, *235*, 1478-1484.
(6) Lightner, D. A.; Gawroński, J. K.; Gawrońska, K. *J. Am. Chem. Soc.* **1985**, *107*, 2456-2461.
(7) For leading references, see: Lightner, D. A.; Reisinger, M.; Landen, G. L. *J. Biol. Chem.* **1986**, *261*, 6034-6038.

0002-7863/87/1509-6354$01.50/0